

# Optical Properties of the Synthesized $\text{Cr}_2\text{S}_3$ Nanoparticles Embedded in Polyvinyl Alcohol

Omed Gh. Abdullah, Dana A. Tahir and Dlear R. Saber

Department of Physics, Faculty of Science and Science Education, School of Science, University of Sulaimani  
Sulaimani, Kurdistan Region - F.R. Iraq

**Abstract**—Polyvinyl alcohol (PVA) based nanocomposite, with different concentrations of chromium sulfide  $\text{Cr}_2\text{S}_3$  nanoparticles, were prepared by reduction of  $\text{Cr}(\text{NO}_3)_3$  and  $\text{Na}_2\text{S}$  in an aqueous PVA solution, using the chemical reduction rate, and casting technique. Effect of  $\text{Cr}_2\text{S}_3$  nanoparticles on optical parameters such as absorbance, absorption coefficient, refractive index, and extinction coefficient have been investigated using UV-Visible spectroscopy. The study reveals that all these parameters are affected by the  $\text{Cr}_2\text{S}_3$  nanoparticles concentration. The study has been also extended to investigate the changes in the optical band gap energies, the band tail width for the samples using Tauc and Urbach relations respectively. The optical energy band gap reduced from (6.17 eV) for pure PVA to (4.14 eV) for 0.04M  $\text{Cr}_2\text{S}_3$ ; while the Urbach tail increased from (0.216 eV) for pure PVA to (0.523 eV) for 0.04M  $\text{Cr}_2\text{S}_3$ . The significant change of the optical properties of PVA with embedded  $\text{Cr}_2\text{S}_3$  nanoparticles suggested their applicability in optical devices.

**Index Terms**— $\text{Cr}_2\text{S}_3$  nanoparticles, filler effect, optical properties, polymer nanocomposite, solution cast technique.

## I. INTRODUCTION

In the past several years, considerable researches have been carried out focusing on the synthesis of the polymer nanocomposite materials with various nanoparticle filler to understanding their physical and chemical properties. By combining polymer and nanoparticle, the resulting composites can possess advantages of both organic polymers and inorganic nanoparticle (Jeon and Baek, 2010). Incorporating a small amount of nano-sized fillers into the polymer matrix, could lead to a significant change in optical, electrical, and mechanical properties (Ayandele, et al. 2012).

Optical properties of different polymers based nanocomposite have received considerable attention in recent

literatures (Liu, et al. 2007; Luo, et al. 2007), it is still meaningful to extend the research on such materials as a promising material for sensors, rechargeable batteries, optoelectronics applications such as light emitting diodes LEDs, and electromagnetic interference shielding (Gurunathan, et al., 1999).

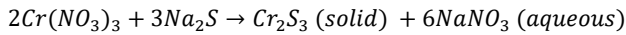
Due to their superior physical and chemical properties, polyvinyl alcohol (PVA) based nanocomposite, has attracted more attention among the other organic nanocomposite (Abdullah, et al., 2011). Major characteristics of PVA include excellent film forming capacity, good transparency, high tensile strength, tear and chemical resistance, and good insulating material which makes important for many applications in industry (Yang and Wu 2009; Gautam and Ram 2010; Ravi, et al., 2011).

The investigation of optical absorption, especially, the absorption edge, the band gap energy, and the band tail of localized state is importance for different applications (Deshmukh, et al., 2008; Abdullah, et al., 2011).

In the present work, an aqueous solution of PVA used as host matrix for  $\text{Cr}(\text{NO}_3)_3$ : $\text{Na}_2\text{S}$  reaction to produce nano  $\text{Cr}_2\text{S}_3$ /polymer nanocomposite. The characterization and analysis focused on the influence of  $\text{Cr}_2\text{S}_3$  nanoparticle concentration on the optical parameters of the PVA, to optimize the optical properties for desired applications.

## II. MATERIALS AND METHODS

The homogeneous and transparent solution of polyvinyl alcohol (PVA) was prepared by dissolving (2 gm) of low molecular PVA supplied by Alfa Aesar in 50 ml distilled water using a hot plate magnetic stirrer at 90°C for 1 hr. Chromium nitrate  $\text{Cr}(\text{NO}_3)_3$  (molar mass=238.0108 g/Mol.) and Sodium sulfide  $\text{Na}_2\text{S}$  (molar mass=78.0445 g/Mol.) as  $\text{Cr}^{3+}$  and  $\text{S}^{2-}$  ion source respectively, were dissolved in the 5 mL distilled water separately with different molar concentrations (0.00, 0.01, 0.02, 0.03 and 0.04) at ambient temperature. Then  $\text{Cr}(\text{NO}_3)_3$ , and  $\text{NaS}$  solution with ration 2:3, prepared separately and then added drop by drop to the homogeneous solution of PVA at 40°C. For maximum dispersion, the solution was further stirred for 30 minutes without heating. The production process of  $\text{Cr}_2\text{S}_3$  was according to the following reaction:



The mixture of the prepared solution was casted onto a clean plastic Petri dish and allowed to evaporate slowly at room temperature for two weeks. For continuous drying with blue silica gel, the produced films transferred into desiccators. The prepared films have a uniform thickness in the range of (0.17-0.21) mm. The measurements of absorbance and transmittance spectra of the prepared films were carried out at room temperature using double beam Ultraviolet-visible spectrophotometer (Lambda-25) in the wavelength region of (190-1100) nm.

### III. RESULTS AND DISCUSSION

Fig. 1 shows the absorption spectra of the PVA films filled with different concentrations of  $Cr_2S_3$ . The pure PVA film exhibits a main peak at 284 nm as well as a shoulder at about 333 nm. The main peak attributed to the absorption of the carbonyl group, while the shoulder assigned to the  $-(CH=CH)3CO-$  structure (El-Khodary, 2010; Abdullah, et al. 2013).

The nanocomposite films with different contents of  $Cr_2S_3$ , showed two broad bands approximately centered at (415 and 570)nm in the visible region, which are related to surface plasmon resonance (SPR) that correlated to the  $Cr_2S_3$  nanoparticle (Massoumi, et al. 2013). The SPR bands of the nanoparticle are sensitive to the shape and size of the particle size (Noguez 2007; El-Brollosy, et al. 2008). The intensity of these bands increases with increasing salt concentration providing evidence for the incorporation of the  $Cr_2S_3$  into PVA matrix. The observed blue shift of the two bands comparing to the Cr(III) spectra (421 and 592) nm in reference (Subramaniam, et al. 2013), attribute to the quantum confinement effect (Seoudi, et al. 2012), Whereas the shift in onset of absorption spectra towards the higher wavelength upon increasing  $Cr_2S_3$  confirm the increase of the average size of nanoparticles (Deshmukh, et al. 2012).

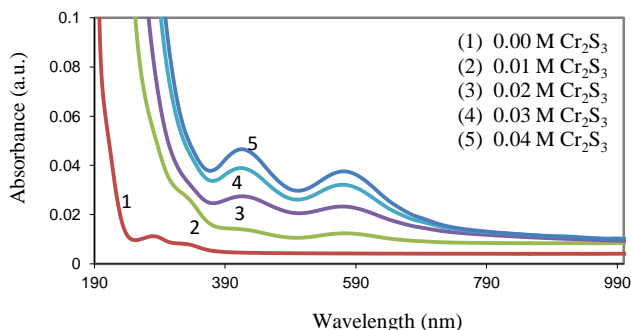


Fig. 1. The absorption spectra of pure PVA, and PVA/ $Cr_2S_3$  nanocomposite.

The optical absorption coefficient  $\alpha$  is defined as the ability of a material to absorb light of a given wavelength; it provides the most valuable optical information such as the electronic band structure and the optical energy band gap for material

identification. The variation of optical absorption coefficient  $\alpha$  with wavelength can be calculated from the optical absorption spectrum using the Beer-Lambert's relation (Abdullah, et al. 2013; Ballato, et al. 2003):

$$\alpha = \frac{2.303A}{d} \quad (1)$$

where,  $d$  is the sample thickness in (cm), and  $A$  is absorbance defined as  $\log(I_o/I)$  where  $I_o$  and  $I$  are the intensities of the incident and transmitted beam light respectively (El-Khodary, 2010).

Figure 2 shows the dependence of the absorption coefficient on the photon energy for pure PVA sample and the  $Cr_2S_3$ /PVA nanocomposite samples. The absorption coefficient increases with the increasing of  $Cr_2S_3$  concentration.

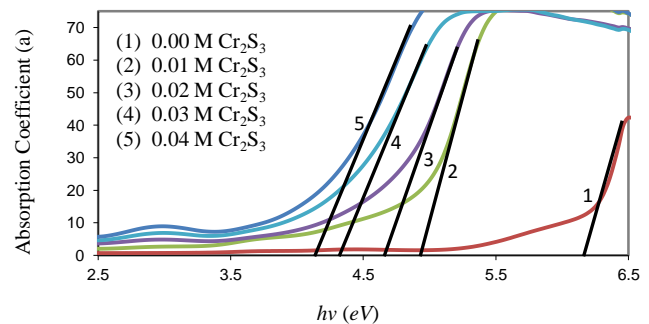


Fig.2. The optical absorption coefficient for pure PVA and PVA/ $Cr_2S_3$  nanocomposite.

The refractive index is a fundamental characterization of the optical study, the values of refractive index ( $n$ ) could be determined from the optical reflectance ( $R$ ) of the investigated films, using the Fresnel formulae as follows (Yakuphanoglu, et al. 2007):

$$n = \left( \frac{1+R}{1-R} \right) + \left[ \frac{4R}{(1-R)^2} - k^2 \right]^{1/2} \quad (2)$$

where ( $k = \alpha\lambda/4\pi$ ) is the extinction coefficient,  $\lambda$  is the incident photon wavelength.

Fig. 3 shows the variation of the refractive index of nanocomposites as the function of photon energy. The refractive index increases as a result of increasing the concentration of  $Cr_2S_3$  nano-filler, this behavior can be attributed to the increasing of the packing density of nanocomposite as a result of filler content (Amma, et al., 2005).

The variation of the extinction coefficient ( $k$ ) with photon energy for PVA/ $Cr_2S_3$  nanocomposites is as shown in Fig.4. The extinction coefficient increases with increasing of  $Cr_2S_3$  nanoparticles concentration. This behavior of extinction coefficient can be ascribed to the variation of the absorption coefficient since  $k$  directly proportional to  $\alpha$ .

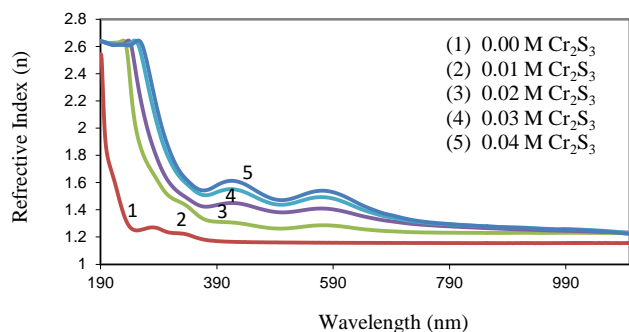


Fig. 3. The refraction index of PVA/Cr<sub>2</sub>S<sub>3</sub> nanocomposite as a function wavelength.

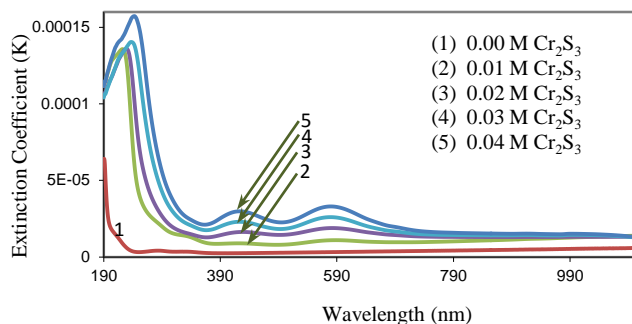


Fig. 4. The extinction coefficient for PVA/Cr<sub>2</sub>S<sub>3</sub> nanocomposite as a function of wavelength.

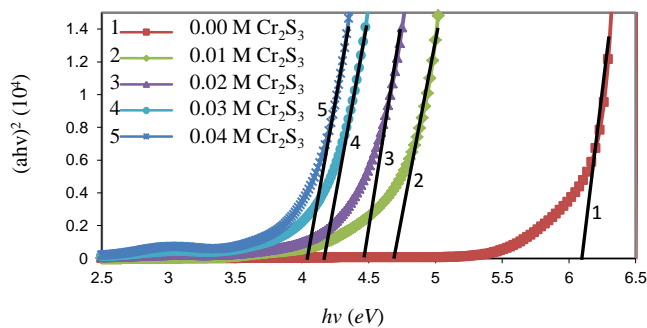
The optical absorption spectra for the near absorption edge, can be used to determine the nature of the transition (direct or indirect), and the value of the optical energy band gap  $E_g$ . The present optical data can be investigated in view of the models proposed by Tauc (1970);

$$\alpha = B \frac{(hv - E_g)^r}{hv} \quad (3)$$

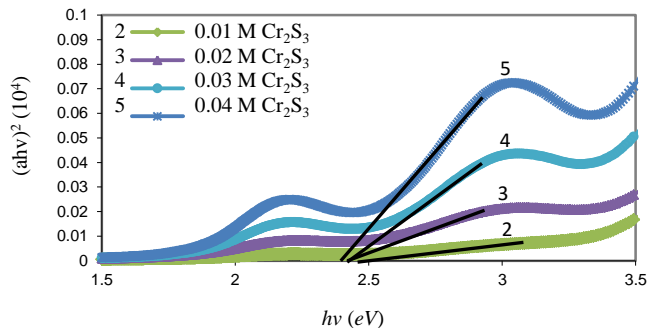
Where,  $B$  is a constant,  $hv$  is the incident photon energy, and  $r$  is the power that characterizes the optical transition process. The exponent  $r$  determines the type of electronic transitions causing optical absorption, it can take values 1/2, 3/2, 2 or 3 for transitions designated as direct allowed, direct forbidden, indirect allowed, and indirect forbidden respectively (El-Khodary, 2010).

Figure 5 shows the plots of  $(\alpha hv)^{1/2}$  versus the photon energy ( $hv$ ) for the present experimental data near the absorption edge. The linearity of the data suggests the presence of indirect allowed transitions in the PVA and its composite. Extrapolation of the linear portion of the plots to the abscissa yields the indirect optical energy band gaps of PVA/Cr<sub>2</sub>S<sub>3</sub> nanocomposite and Cr<sub>2</sub>S<sub>3</sub> nanoparticles. The values of optical energy band gaps are given in Table 1. The obtained data revealed that the optical energy band gap decrease significantly with increasing nano Cr<sub>2</sub>S<sub>3</sub> concentration, which may be explained on the basis of the fact that the incorporation of small amounts of dopant forms

charge transfer complexes in the host matrix (Abdullah, et al. 2013). These charge transfer complexes increase the electrical conductivity by providing additional charges, this result in a decrease of the optical energy band gap, by facilitating the transfer of charge carrier between the localized states (Abdelrazek, et al., 2013; Sangawar, et al., 2007).



(a)



(b)

Fig. 5.  $(\alpha hv)^{1/2}$  versus photon energy ( $hv$ ) for; (a) PVA/Cr<sub>2</sub>S<sub>3</sub> nanocomposite and (b) Cr<sub>2</sub>S<sub>3</sub> nanoparticles.

The width of the localized tail states in the forbidden gap (Urbach tail), is an indicator of the defect levels in the forbidden band gap (El-Khodary, 2010). The absorption coefficients just below the fundamental gap can be used to calculate the Urbach energy using following relations (Urbach 1953):

$$\alpha = \alpha_o \exp\left(\frac{hv}{E_u}\right) \quad (4)$$

where  $\alpha_o$  is a constant and  $E_u$  is the Urbach energy interpreted as the width of the tails of the localized state in the forbidden gap. The exponential dependence of  $\alpha$  on the photon energy ( $hv$ ) for the investigated samples indicates that it obeys Urbach's formula. The Urbach plot is presented in Fig.6, in which the natural logarithm of absorption coefficient  $\alpha$  was plotted as a function of photon energy ( $hv$ ). The magnitudes of the Urbach energy  $E_u$  were estimated, by taking the reciprocal of the slopes of the linear portion. The optical band gap and band tails of the localized state of the samples are summarized in Table I.

The Urbach energy tail  $E_u$  was found to be proportional to the  $\text{Cr}_2\text{S}_3$  concentration in PVA/ $\text{Cr}_2\text{S}_3$  nanocomposites. Increasing  $\text{Cr}_2\text{S}_3$  content may cause the localized states to overlap and extend into the mobility gap in the polymeric matrix (Reda, and Zahrani 2012; Abdelrazek, et al., 2013). The observed increase in the Urbach energy with increasing  $\text{Cr}_2\text{S}_3$  concentration, correlated with the decrease of the energy gap, and absorption edge accordingly.

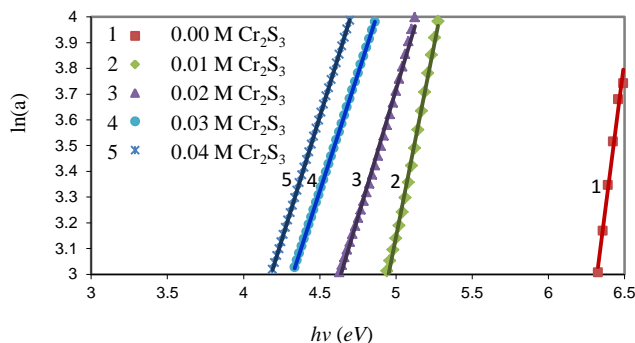


Fig. 6. The relation between  $\ln(a)$  and photon energy ( $h\nu$ ), for PVA at different  $\text{Cr}_2\text{S}_3$  nanoparticles concentration.

TABLE I

VALUES OF THE ABSORPTION EDGE ( $E_e$ ), DIRECT ENERGY GAP ( $E_g$ ), FOR PVA/ $\text{Cr}_2\text{S}_3$  NANOCOMPOSITE, ENERGY GAP OF  $\text{Cr}_2\text{S}_3$  NANOPARTICLES ( $E_n$ ) AND BAND TAIL ENERGY ( $E_u$ )

$\text{Cr}_2\text{S}_3$ (M)	$E_e$ (eV)	$E_d$ (eV)	$E_n$ (eV)	$E_u$ (eV)
0.00	6.17	6.10	-	0.216
0.01	4.93	4.69	2.50	0.336
0.02	4.67	4.47	2.44	0.503
0.03	4.33	4.17	2.43	0.550
0.04	4.13	4.04	2.40	0.523

#### IV. CONCLUSIONS

Chemical reduction rate and solution cast method and have been used to prepare polymer nanocomposite films of PVA with different concentrations of  $\text{Cr}_2\text{S}_3$  nanoparticles, and their optical properties have been investigated. The absorbance, absorption coefficient, extinction coefficient, and refraction index of  $\text{Cr}_2\text{S}_3$  doped PVA films increase with increasing of doping concentration. The decreasing trend of the optical band gap of nanocomposite, with increasing the  $\text{Cr}_2\text{S}_3$  nanoparticles concentration, was attributed to formation charge transfer complexes, while the increase of Urbach energy suggests the presence of the deep localized state in the band gaps. The decrease of the optical band gap of nanoparticle upon increasing  $\text{Cr}_2\text{S}_3$  additions suggested the smaller  $\text{Cr}_2\text{S}_3$  nanoparticles were synthesized in a small amount of Cr salt.

#### ACKNOWLEDGMENT

The authors express their gratefulness to the School of Science, University of Sulaimani, for the facilities and financial support.

#### REFERENCES

- Abdelrazek, E.M., Ragab, H.M. and Abdelaziz M., 2013. Physical characterization of poly (vinyl pyrrolidone) and gelatin blend films doped with magnesium chloride. *Plastic and Polymer Technology*, 2(1), pp.1-8.
- Abdullah, O.G. and Aziz, B.K., 2011. Effect of kaolin light concentration on optical characteristic of PVA films. *Asian Transactions on Science & Technology*, 1(4), pp.12-15.
- Abdullah, O.G., Aziz, B.K. and Salh D.M., 2013. Structural and optical properties of PVA: $\text{Na}_2\text{S}_2\text{O}_3$  polymer electrolytes films. *Indian Journal of Applied Research*, 3(11), pp.477-480.
- Amma D.S.D., Vaidyan V.K. and Manoj P.K., 2005. Structural, electrical and optical studies on chemically deposited tin oxide films from inorganic precursors. *Materials Chemistry and Physics*, 93(1), pp.194-201.
- Ayandele, E., Sarkar B. and Alexandridis P., 2012. Polyhedral oligomeric silsesquioxane (POSS)-containing polymer nanocomposites. *Nanomaterials*, 2(4), pp.445-475.
- Ballato, J., Foulger S. and Smith D.W., 2003. Optical properties of perfluorocyclobutyl polymers. *Journal of the Optical Society of America B*, 20(9), pp.1838-1843.
- Deshmukh K., Mukherjee M. and Bhushan S., 2012. Structural and optical studies on La doped CdS nanocrystalline films. *Turk J. Phys.*, 36, pp.9-21.
- Deshmukh, S.H., Burghate, D.K., Shilaskar S.N., Chaudhari G.N. and Deshmukh P.T., 2008. Optical properties of polyaniline doped PVC-PMMA thin films. *Indian Journal of Pure and Applied Physics*, 46, pp.344-348.
- El-Brolossy T.A., Abdallah T., Mohamed M.B., Abdallah S., Easawi K., Negm S., Talaat H., 2008. Shape and size dependence of the surface plasmon resonance of gold nanoparticles studied by Photoacoustic technique. *Eur. Phys. J. Special Topics*, 153(1), pp.361-364.
- El-Khodary, A., 2010. Evolution of the optical, magnetic and morphological properties of PVA films filled with  $\text{CuSO}_4$ . *Physica B: Condensed Matter*, 405(16), pp.4301-4308.
- Gautam, A. and Ram S., 2010. Preparation and thermomechanical properties of Ag-PVA nanocomposite films. *Materials Chemistry and Physics*, 119(1-2) pp.266-271.
- Gurunathan, K., Murugan, A.V., Marimuthu, R., Mulik, U.P. and Amalnerkar D.P., 1999. Electrochemically synthesised conducting polymeric materials for applications towards technology in electronics, optoelectronics and energy storage devices. *Materials Chemistry and Physics*, 61(3), pp.173-191.
- Jeon, I.Y. and Baek J.B., 2010. Nanocomposites derived from polymers and inorganic nanoparticles. *Materials*, 3(6), pp.3654-3674.
- Liu, J., Shao, S.Y., Chen, L., Xie, Z.Y., Cheng, Y.X., Geng, Y.H., Wang, L.X., Jing, X.B., Wang, F.S., 2007. White electroluminescence from a single polymer system: improved performance by means of enhanced efficiency and red-shifted luminescence of the blue-light-emitting species. *Advanced Materials*, 19(14), pp.1859-1863.
- Luo, J., Li X., Hou, Q., Peng, J.B., Yang, W. and Cao, Y., 2007. High-efficiency white-light emission from a single copolymer: fluorescent blue, green, and red chromophores on a conjugated polymer backbone. *Advanced Materials*, 19(8), pp.1113-1117.
- Massoumi, B., Fathalipour, S., Massoudi, A., Hassanzadeh, M. and Entezami, A.A., 2013. Ag/polyaniline nanocomposites: synthesize, characterization, and application to the detection of dopamine and tyrosine. *Journal of Applied Polymer Science*, 130(4), pp.2780-2789.
- Noguez, C., 2007. Surface plasmons on metal nanoparticles: the influence of shape and physical environment. *J. Phys. Chem. C*, 111(10), pp.3806-3819.
- Ravi, M., Pavani, Y., Kumar, K.K., Bhavai, S., Sharma, A.K. and Rao, V.V.R.N., 2011. Studies on electrical and dielectric properties of PVP: $\text{KBrO}_4$  complexed polymer electrolyte films. *Materials Chemistry and Physics*, 130(1-2), pp.442-448.
- Reda, S.M. and Al-Zahrani, A.A., 2012. Ponceau 2R doped poly (ST/MMA) as fluorescent solar collectors and evaluation effect of matrix on their field performance. *Open Journal of Energy Efficiency*, 1(3), pp.62-74.

Sangawar, V.S., Dhokne, R.J., Ubale, A.U., Chikhalikar, P.S. and Meshram S.D., 2007. Structural characterization and thermally stimulated discharge conductivity (TSDC) study in polymer thin films. *Bulletin of Materials Science*, 30(2), pp.163-166.

Seoudi, R., El-Bailly, A.B., Eisa, W., Shabaka, A.A., Soliman, S.I., Abd El Hamid, R.K. and Ramadan, R.A., 2012. Synthesis, optical and dielectric properties of (PVA-CdS) nanocomposites. *Journal of Applied Sciences Research*, 8(2), pp.658-667.

Subramaniam, P. and Selvi, N.T., 2013. Spectral evidence for the one-step three-electron oxidation of phenylsufinylacetic acid and oxalic acid by Cr(VI). *American Journal of Analytical Chemistry*, 4(10), pp.20-29.

Taucm J., Menth A. and Wood, D.L., 1970. Optical and magnetic investigations of the localized states in semiconducting glasses. *Physical Review Letters*, 25(11), pp.749-752.

Urbach, F., 1953. The long-wavelength edge of photographic sensitivity and of the electronic absorption of solids. *Phys. Rev.*, 92(5), pp.1324-1324.

Yakuphanoglu, F., Kandaz, M., Yarasir, M.N. and Senkal F.B., 2007. Electrical transport and optical properties of an organic semiconductor based on phthalocyanine. *Physica B: Condensed Matter*, 393(1-2), pp.235-238.

Yang, C.C. and Wu, G.M., 2009. Study of microporous PVA/PVC composite polymer membrane and it application to MnO<sub>2</sub> capacitors. *Materials Chemistry and Physics*, 114(2-3), pp.948-955.